

Effects of multiple sources of genetic drift on pathogen variation within hosts

David A. Kennedy^{1,2} and Greg Dwyer^{2,*}

¹Center for Infectious Disease Dynamics, Pennsylvania State University

²Ecology and Evolution, University of Chicago

*To whom correspondence should be addressed: gdwyer@uchicago.edu.

Running title: Multiscale drift affects pathogen variation

Keywords: host-pathogen ecology, genetic drift, nested model, sequence data, within-host diversity, phylodynamic inference, population bottleneck, demographic stochasticity

January 13, 2018

1 **Abstract**

2 Changes in pathogen genetic variation within hosts alter the severity and spread of infectious
3 diseases, with important implications for clinical disease and public health. Genetic drift
4 may play a strong role in shaping pathogen variation, but analyses of drift in pathogens have
5 oversimplified pathogen population dynamics, either by considering dynamics only at a single
6 scale (within hosts, between hosts), or by making drastic simplifying assumptions (host immune
7 systems can be ignored, transmission bottlenecks are complete). Moreover, previous studies
8 used genetic data to infer the strength of genetic drift, whereas we test whether the genetic
9 drift imposed by pathogen population processes can be used to explain genetic data. We first
10 constructed and parameterized a mathematical model of gypsy moth baculovirus dynamics that
11 allows genetic drift to act within and between hosts. We then quantified the genome-wide
12 diversity of baculovirus populations within each of 143 field-collected gypsy moth larvae
13 using Illumina sequencing. Finally, we determined whether the genetic drift imposed by
14 host-pathogen population dynamics in our model explains the levels of pathogen diversity in
15 our data. We found that when the model allows drift to act at multiple scales, including within
16 hosts, between hosts, and between years, it can accurately reproduce the data, but when the
17 effects of drift are simplified by neglecting transmission bottlenecks and stochastic variation
18 in virus replication within hosts, the model fails. A *de novo* mutation model and a purifying
19 selection model similarly fail to explain the data. Our results show that genetic drift can play
20 a strong role in determining pathogen variation, and that mathematical models that account for
21 pathogen population growth at multiple scales of biological organization can be used to explain
22 this variation.

23 **Introduction**

24 Pathogen genetic variation can have important consequences for human health, in both clinical
25 and epidemiological settings (Alizon et al. 2011). In particular, high variation within hosts
26 can lead to severe disease symptoms within individuals, and rapid disease transmission within
27 populations (Read and Taylor 2001; Vignuzzi et al. 2006). An understanding of the mechanisms
28 determining pathogen variation might therefore lead to novel interventions, reducing the toll of
29 infectious diseases. Development of such an understanding requires quantification of the effects
30 of population processes on pathogen genetic variation, in turn requiring mathematical models
31 that relate population processes to genetic change.

32 Such models, however, tend to greatly simplify pathogen biology. Selection-mutation
33 models, for example, often assume that pathogen populations are effectively infinite
34 (Lorenzo-Redondo et al. 2016). Models that allow pathogen population sizes to be finite
35 typically neglect pathogen population processes either within hosts in acute infections (Koelle
36 et al. 2006), or between hosts in chronic infections (Pennings et al. 2014). Models that attempt to
37 capture both of these scales of disease dynamics have assumed either that pathogen population
38 growth within hosts is very simple (Klinkenberg et al. 2017), or that pathogen bottlenecks at
39 transmission are complete (Didelot et al. 2014; Klinkenberg et al. 2017; Ypma et al. 2013),
40 so that every infection begins as a clonal lineage. These simplifications could strongly alter
41 conclusions about the effects of genetic drift on pathogen diversity, and indeed have been
42 highlighted as key challenges in phylodynamic inference (Frost et al. 2015).

43 Genetic drift is a change in an allele's frequency due to the chance events that befall
44 individuals. The effects of drift are thus strongest in small populations, in which a few events
45 can have a large impact (Nagylaki 1992). The high population sizes typical of severe infections
46 have led some authors to argue that drift has little effect on pathogens (Kouyos et al. 2006;

47 Maldarelli et al. 2013), but pathogen population sizes typically fluctuate by several orders
48 of magnitude over the course of infection and transmission. It therefore seems likely that,
49 when pathogen populations are small and variable, pathogen genetic variation will be strongly
50 affected by drift. Indeed, analyses that allow for finite population sizes have shown that drift
51 has at least weak effects on some pathogens (Pennings et al. 2014).

52 New infections are typically initiated by small pathogen population sizes within hosts
53 (Gutiérrez et al. 2012), leading to bottlenecks at the time of transmission that may drive genetic
54 drift. Pathogen population sizes within hosts can also remain small for long periods following
55 exposure (Kennedy et al. 2014). In small populations, chance events such as the timing of
56 reproduction can strongly influence population growth, a phenomenon known as “demographic
57 stochasticity” (Kot 2001). When the effects of demographic stochasticity are strong, chance
58 may allow some virus strains to replicate and survive while others go extinct, providing a second
59 source of genetic drift that we refer to as “replicative drift”. Note that we use the term “strain”
60 to mean a population of pathogen particles that have identical genetic sequences.

61 Many previous studies of genetic drift in pathogens have focused only on population
62 processes that operate within hosts, either during experiments with model organisms, or during
63 the treatment of human patients (Abel et al. 2015; Gutiérrez et al. 2012). Pathogen variation in
64 nature, however, is also affected by processes that operate at the host population level, such as
65 fluctuating infection rates during epidemics (Grenfell et al. 2004). Studies of Ebola (Azarian
66 et al. 2015) and tuberculosis (Lee et al. 2015), for example, have shown that much of the
67 variation present at the population level often cannot be explained by natural selection, and
68 must instead be due to neutral processes that presumably include genetic drift.

69 Genetic drift in pathogens may thus be driven by population processes at multiple scales.
70 These multiple scales can be incorporated into a single framework by constructing “nested”
71 models, in which sub-models of within-host pathogen population growth are nested in models

72 of between-host pathogen transmission (Mideo et al. 2008). The computing resources necessary
73 to analyze such complex models have only become available recently, however, and so it has not
74 been clear whether sufficient data exist to test nested models of drift (Gog et al. 2015). Indeed,
75 even for models that assume that the strength of drift is constant across hosts, robust tests of the
76 model predictions require both genetic data and mechanistic epidemiological models (Didelot
77 et al. 2014), a combination that is rarely available. Whether nested models can be of practical
78 use for understanding pathogen genetic variation in nature is therefore unclear.

79 For baculovirus diseases of insects, pathogen population processes have been intensively
80 studied at both the host population level (Elder 2013), and at the individual host level
81 (Kennedy et al. 2014). Baculoviruses cause severe epizootics (= epidemics in animals) in
82 many insects (Moreau and Lucarotti 2007), including economically important pest species
83 such as the gypsy moth (*Lymantria dispar*) that we study here (Woods and Elkinton 1987).
84 Collection and rearing protocols for the gypsy moth have long been standardized (Elkinton
85 and Liebhold 1990), and so previous studies of the gypsy moth baculovirus *Lymantria*
86 *dispar* multiple nucleopolyhedrovirus (LdMNPV) have produced parameter estimates for both
87 within-host (Kennedy et al. 2015) and between-host (Elder et al. 2008, 2013; Fuller et al. 2012)
88 models. Moreover, collection of large numbers of virus-infected individuals is straightforward
89 (Woods and Elkinton 1987), making it possible to use high-throughput sequencing methods to
90 characterize pathogen diversity across many virus-infected hosts. Here we use a combination of
91 whole-genome sequencing and parameterized, nested models to quantify the effects of genetic
92 drift on the gypsy moth baculovirus. We show that a mechanistic model of genetic drift can
93 explain variation in this pathogen, but only if the model takes into account the effects of drift at
94 multiple scales of biological organization.

95 **Results**

96 Sequencing the virus populations from each of 143 field-collected insects showed that there is
97 substantial genetic variation in baculovirus populations between hosts. We generated consensus
98 sequences for each of our 143 samples (see Supplemental Information A), and comparisons
99 between consensus sequences identified 712 segregating sites at the between host scale (defined
100 as sites where alternative variants were the consensus in more than 6 samples ($\approx 5\%$)). These
101 sites correspond to approximately 0.4% of the genome. Analysis of the variation at these
102 712 sites within each sampled virus population showed that these sites were polymorphic in
103 some hosts but not others, which might occur if some hosts were exposed to multiple strains
104 of virus, while others were exposed to only a single strain. We summarize genetic variation
105 within hosts using mean nucleotide diversity (Nei and Li 1979), the probability that two
106 randomly selected alleles at a segregating site are different (Supplemental Information A). Our
107 conclusions were nevertheless unchanged when we used alternative metrics of diversity, such
108 as the proportion of polymorphic loci, the effective number of alleles, or the relative nucleotide
109 diversity (Supplemental Information I).

110 Measured across the consensus sequences of our 143 samples, nucleotide diversity at our
111 712 segregating sites was quite high at 0.404. Within samples, nucleotide diversity at these
112 same sites ranged from 0.002 to 0.284 (mean = 0.072, s.d. = 0.077, Supplemental Information
113 B). Overall nucleotide diversity within samples ranged from 0.001 to 0.003, with a mean of
114 0.001. In Supplemental Information B, we show that these values imply that a large fraction of
115 nucleotide diversity within hosts can be explained by just 712 segregating sites, or 0.4% of the
116 genome.

117 Together, these patterns suggest that substantial pathogen diversity within hosts is likely
118 acquired from the exposure of host insects to multiple virus strains. If diversity had instead

119 been generated by *de novo* mutation, nucleotide diversity between samples would have
120 been less variable (Supplemental Information E), and polymorphism would have likely been
121 spread across many sites, including sites that were not polymorphic at the population level.
122 Immune-system mediated diversifying selection is also an unlikely explanation, because insects
123 lack clonal immune cell expansion (Vilmos and Kurucz 1998), because immune cell expansion
124 does not explain why some hosts have substantially more pathogen diversity than others, and
125 because we found no evidence of diversifying selection in our sequence data (Supplemental
126 Information H). Negative correlations between host families in susceptibility to different
127 pathogen genotypes constitute yet a third unlikely explanation, because in the gypsy moth such
128 correlations are positive (Hudson et al. 2016). Migration of virus or infected larvae from nearby
129 locations with different virus strains similarly cannot explain the data, because population
130 structure in the gypsy moth virus is minimal (Fujita 2007, Supplemental Information A).

131 Genetic drift, however, can explain the data, but only if we allow for effects of population
132 processes at multiple scales of biological organization. To explain why, we first use a
133 nested model of pathogen population dynamics (fig. 1) to show how genetic drift in pathogen
134 populations may operate at three scales; within hosts, within epizootics, and between years. We
135 then show that the model can only explain the data if it includes effects of drift both during
136 transmission bottlenecks and virus growth within hosts.

137 Simulations of our within-host model show that the combination of transmission bottlenecks
138 and replicative drift can substantially reduce pathogen diversity within hosts (fig. 2A-C).
139 Demographic stochasticity, which is manifest in the figure as jaggedness in the model
140 trajectories, is strongest shortly after exposure, when the pathogen population size is small. This
141 stochasticity generates variability in the time to host death, and it also drives replicative drift.
142 Comparing this model to a linear birth-death model (Supplemental Information C) shows that
143 the immune system substantially slows the growth of the virus population early in the infection,

144 which strengthens the effects of replicative drift.

145 Overwintered virus infects hatchlings during the initial emergence of hosts from eggs,
146 an effect that is apparent in our simulations of the epizootic model (fig. 2D-E). After the
147 overwintered virus decays, there is a short period when cadavers are rare, such that the vast
148 majority of virus is present only within exposed larvae. When these exposed larvae die, the
149 virus that they release is transmitted to new larvae feeding on foliage. During this time, the
150 relative frequencies of different virus strains consumed by larvae can fluctuate strongly due to
151 the drift that occurs when cadavers are rare. Low densities of cadavers can thus alter the relative
152 frequency of strains within hosts. In the figure, the initial host population consists of more
153 than 10,000 hosts, reflecting the high densities at which baculovirus epizootics occur in insect
154 populations in nature (Moreau and Lucarotti 2007). Demographic stochasticity nevertheless
155 influences the composition of virus strains near the end of the epizootic, when the pathogen
156 population begins to die out, in turn allowing drift to influence which virus strains cause
157 infections within hosts.

158 Over longer time periods, fluctuations at the population scale (fig. 2F) produce
159 host-pathogen cycles that match the dynamics of gypsy moth outbreaks in nature (Dwyer et al.
160 2000; Elder et al. 2008). These large fluctuations can drive changes in the relative frequency
161 of pathogen strains, especially when pathogen population sizes and overall infection rates are
162 at their lowest, in the troughs between host population peaks. Host-pathogen population cycles
163 in our model thus further strengthen the effects of genetic drift on the pathogen.

164 Our combined model therefore shows that drift can act both within and between hosts, and
165 at time scales ranging from hours to decades. To test the model, we compared its predictions of
166 nucleotide diversity to the levels of nucleotide diversity in our data. To test whether the data can
167 be explained equally well by models that neglect one or more sources of drift, we also tested
168 models that eliminated replicative drift, or that eliminated both replicative drift and transmission

169 bottlenecks. Note that it is not possible to construct a model that includes replicative drift but not
170 transmission bottlenecks, because replicative drift requires virus population sizes to be integer
171 values, and forcing the virus population to have an integer value necessarily imposes a form
172 of bottleneck. Also, to test whether the data are better explained by selection than by drift, we
173 constructed a model that allows for purifying selection to act within hosts, but that lacks both
174 replicative drift and transmission bottlenecks.

175 These comparisons show that only the model that includes both replicative drift and
176 bottlenecks can explain the data (fig. 3). The neutral model that includes only drift at the
177 host-population scale predicts within-host diversity levels that are much higher and much less
178 variable than in the data. The model that includes population-scale drift and bottlenecks but not
179 replicative drift, and the model that includes purifying selection but not transmission bottlenecks
180 or replicative drift both correctly predict that there will be substantial variation across hosts,
181 but they predict diversity levels that are much higher than in the data. In Supplemental
182 Information D and G, we show that these qualitative conclusions are robust across parameter
183 values that determine bottleneck severity and selection intensity. In contrast, the model that
184 includes replicative drift and transmission bottlenecks accurately predicts the entire distribution
185 of diversity levels seen in the data. This visual impression is strongly confirmed by differences
186 in the Monte Carlo estimates of the likelihood scores across models (Supplemental Information
187 F: neutral model with neither bottlenecks nor replicative drift, median log mean likelihood
188 = -503.2 ; purifying selection model, median log mean likelihood = -353.1 , neutral model
189 with bottlenecks but not replicative drift, median log mean likelihood = -266.7 ; neutral model
190 with both bottlenecks and replicative drift, median log mean likelihood = -63.9). Because no
191 parameters were fit to the diversity data, we do not need a model complexity penalty, but the
192 difference in the number of parameters across models was in any case dwarfed by the differences
193 in the likelihood scores.

194 Our results thus show that a model that accounts for the effects of population processes at
195 multiple scales can explain differences in pathogen variation across hosts in the gypsy moth
196 baculovirus. In contrast, models that simplify the effects of genetic drift by ignoring effects
197 of transmission bottlenecks and replicative drift, or that allow for selection but not within host
198 drift, cannot explain the diversity of this pathogen. More broadly, because the model parameters
199 were estimated entirely from experimental data on baculovirus infection rates (Supplemental
200 Information C), we are effectively carrying out cross-validation of the model.

201 The highly skewed distribution of nucleotide diversity apparent in our data can thus be
202 explained by a model that allows for drift at multiple scales, and that includes multiple sources
203 of drift within hosts, but not by simpler models. In addition, fig. 4 shows that the best
204 model can reproduce entire distributions of diversity within individual hosts. Allele-frequency
205 distributions in the model nevertheless tend to have slightly shorter tails and narrower peaks
206 compared to the data. These mild discrepancies may be partially explained by mutations that
207 occurred during viral passaging or during library preparation, but they can also be explained by
208 small biases introduced during the mapping of our short sequence reads to the reference genome
209 (Supplemental Information J). The data therefore do not reject the model.

210 Our virus samples were collected at times of peak or near-peak gypsy moth densities, which
211 are the only times at which large numbers of larvae can be collected easily, and so the data
212 do not directly show how changes in pathogen population size at the host-population scale
213 affect pathogen variation. We therefore used our best model to explore how pathogen variation
214 within hosts will change over the course of the gypsy moth outbreak cycle. Within-host
215 diversity is predicted to be highest just as the host population begins to crash due to the
216 pathogen, after which diversity is predicted to gradually decline until the next outbreak (fig. 5).
217 Reductions in within-host variation due to transmission bottlenecks and replicative drift are
218 thus counter-balanced by increases in within-host variation at the time of host population peaks,

219 due to the high frequency of multiple exposures when host populations are large. Long-term,
220 population-scale processes can therefore also strongly affect within-host variation.

221 **Discussion**

222 A basic prediction of population genetics theory (Nagylaki 1992), and a fundamental
223 assumption of phylodynamic modeling (Grenfell et al. 2004), is that the effects of genetic drift
224 are determined by population processes. Explicit tests of this assumption for infectious diseases,
225 however, are rare. We used a model that was developed and parameterized using non-genetic
226 datasets to show that patterns of genetic diversity in an insect pathogen can be explained by a
227 model that accounts for population processes at multiple scales, but not by models that simplify
228 or neglect the effects of drift. Previous work has attempted to infer disease demography and
229 pathogen evolution from genetic data (Grenfell et al. 2004). Here we instead began with an
230 existing population process model that has already been fit to epidemiological data, and we use
231 it to predict pathogen genetic data. We thus tested the extent to which disease demography can
232 be used to predict neutral pathogen evolution.

233 A simple model of purifying selection was not able to explain the patterns of diversity
234 in our data. Models that instead invoke diversifying selection or more complex patterns of
235 host-specific immune selection might provide reasonable explanations for our data, but such
236 models require extra parameters to account for the costs and benefits of alternative alleles,
237 increasing the complexity of the models (Orr 1998). Moreover, drift is an inherent property
238 of small populations, and so models that invoke selection should still allow for effects of drift
239 if population sizes are small. In our case, complex models of selection were not needed to
240 explain patterns of diversity, suggesting that the effects of selection on our data are weak
241 relative to the effects of drift. Selection may nevertheless be necessary to explain variation

242 in other pathogens or other datasets. Given that polymorphism has been widely observed
243 in insect baculoviruses (Chateigner et al. 2015; Hodgson et al. 2001), our results suggest
244 that baculoviruses present opportunities to understand the relationship between host-pathogen
245 ecology and pathogen diversity.

246 We have shown that both transmission bottlenecks and replicative drift have detectable
247 impacts on pathogen diversity. Due to the difficulty of separating these effects, previous
248 studies of genetic drift have assumed that bottlenecks are complete (Klinkenberg et al. 2017;
249 Pennings et al. 2014; Ypma et al. 2013), have ignored impacts of key biological processes
250 such as the host immune response (Sobel Leonard et al. 2017), or have summarized the
251 effects of multiple sources of drift with a single parameter, the effective population size
252 N_e (Volz et al. 2017). Similarly, estimates of bottleneck size often combine the effects of
253 transmission bottlenecks and replicative drift into a single estimate of the effective bottleneck,
254 biasing estimates of transmission bottleneck size (Sobel Leonard et al. 2017, Supplemental
255 Information D). Distinguishing between transmission bottlenecks and replicative drift, however,
256 may provide novel insights into disease control strategies. For example, the emergence of
257 resistance to antibiotic drugs might be slowed if drug therapy windows are restricted to periods
258 when the effects of replicative drift are strongest, such as when pathogen populations are small
259 or are turning over rapidly.

260 To show that both transmission bottlenecks and replicative drift play an important role in
261 shaping pathogen diversity within hosts, we have focused our analysis on common variants that
262 cannot be easily explained by *de novo* mutation. Additional variation is nevertheless present
263 (Supplemental Information B). In our case, this other variation occurs at such low levels that it
264 cannot be readily distinguish from sequencing error, but it is almost certainly true that mutation
265 and selection also play roles in shaping total pathogen diversity within hosts. Our argument
266 is therefore not that mutation and selection are unimportant, but instead that transmission

267 bottlenecks and replicative drift can strongly affect pathogen diversity within hosts. In our
268 case, bottlenecks and replicative drift appear to be the main drivers of diversity at sites that
269 segregate at the population level.

270 High-throughput sequencing has revolutionized our ability to measure pathogen variation.
271 It has been used to detect drug-resistance (Mideo et al. 2016), to discover novel viruses in nature
272 (Lipkin and Anthony 2015), and to diagnose disease in clinical settings (Wilson et al. 2014).
273 Our work shows that high throughput sequencing can also provide important insights into the
274 ecology and evolution of host-pathogen interactions, especially when combined with nested
275 disease models. The increasing availability of both parameterized models (Keeling and Rohani
276 2008) and genomic data (Hatherell et al. 2016) suggests that our approach of using genetic data
277 to challenge models of nested disease dynamics may be widely applicable.

278 **Methods**

279 **Model description**

280 The gypsy moth baculovirus LdMNPV, is a double stranded DNA virus belonging to the family
281 *Baculoviridae*. The virus is approximately 161 kb, and like all baculoviruses, it exists in two
282 forms, as an “occlusion body” that is highly stable in the environment due to its protective
283 proteinaceous matrix, and as a “budded virus” that is released from cells during replication
284 within hosts.

285 The gypsy moth baculovirus is transmitted when larvae consume occlusion bodies while
286 feeding on foliage (Elder et al. 2008). If the resulting virus population grows inside the host
287 to a sufficiently large size, the larva dies, releasing new occlusion bodies onto the foliage.
288 These occlusion bodies are then available to be consumed by additional conspecifics (the virus
289 is species specific (Moreau and Lucarotti 2007)), leading to very high infection rates in high

290 density populations (Woods and Elkinton 1987). During the fall and winter, when the insect is
291 in the egg stage, the virus persists beneath egg masses laid on cadavers or other locations where
292 the virus may be protected from degradation by ultraviolet light (Fleming-Davies and Dwyer
293 2015; Murray and Elkinton 1989). Genetic drift in the gypsy moth baculovirus may therefore
294 be affected by population processes at multiple scales, including within individual hosts and
295 across the host population.

296 Exposure to the virus results in an initial population of only a few virus particles (Kennedy
297 et al. 2014; Zwart et al. 2009), and the population size in the host remains small for a substantial
298 period of time following exposure (Kennedy et al. 2014, 2015). Our model of pathogen growth
299 within hosts therefore tracks population sizes from the initial population bottleneck through the
300 stochastic growth of the pathogen population, until death or recovery. Our model thus explicitly
301 includes genetic drift (fig. 1).

302 Our within-host model is based on a birth-death model (Kot 2001), which describes
303 probabilistic changes in population sizes over time. In birth-death models, the probability of
304 a birth or a death in a small period of time increases with the population size (Renshaw 1991).
305 When the population size is small in a birth-death model, it is possible for extinction to occur
306 due to a chance preponderance of deaths over births, even if the per-capita birth rate exceeds
307 the per-capita death rate. Birth-death models are thus well suited to describe the demographic
308 stochasticity that underlies replicative drift.

309 In our within-host birth-death model, pathogen extinction is equivalent to the clearance
310 of the infection by the host. If the pathogen does not go extinct, its population eventually
311 becomes large enough that the effects of stochasticity are negligible (Saaty 1961), leading to
312 host death when the population reaches an upper threshold. In previous work we showed that
313 linear birth-death models are insufficient to explain data on the speed of kill of the gypsy moth
314 baculovirus, whereas models that allow for nonlinearities due to the immune system produce a

315 better explanation for the data (Kennedy et al. 2014).

316 Our within-host model thus describes virus removal as the outcome of a process that begins
317 with the insect's immune system releasing chemicals that active the phenol-oxidase pathway.
318 This release causes virus particles to be encapsulated and destroyed by host immune cells,
319 and it also incapacitates the immune cell (Ashida and Brey 1998; Trudeau et al. 2001). Our
320 model thus follows standard predator-prey-type immune-system models (Alizon and van Baalen
321 2008), in which the pathogen is the prey, and the immune cells are the predator, except that here
322 the immune cells do not reproduce over the timescale of a single infection. The pathogen
323 population in the model may then be driven to zero because of interactions with the host
324 immune system, or it may persist long enough to overwhelm the host immune system, leading
325 to exponential pathogen growth and eventual host death. Which outcome occurs depends on the
326 initial pathogen population size and on demographic stochasticity during the infection.

327 In our model, the initial pathogen population size within a host is drawn from a Poisson
328 distribution (fig. 1, Kennedy et al. 2014). If the infecting cadaver is composed of multiple
329 strains, the model draws an initial population size for each strain from a multinomial
330 distribution, such that the probability of sampling a particular strain from the infecting cadaver
331 depends on the frequency of that strain in the cadaver. This process creates a transmission
332 bottleneck. Next, the model tracks the population size of each virus strain over the course of
333 the infection. Changes in the relative frequencies of these strains over time creates replicative
334 drift. The host dies when the total pathogen population size exceeds an upper threshold. The
335 frequency of virus strains at the time of host death determines the frequency of strains in the
336 newly generated cadaver.

337 We model pathogen dynamics at the scale of the entire host population first by using
338 a stochastic Susceptible-Exposed-Infected-Removed or "SEIR" model to describe epizootics
339 (in our case the infected I class consists of infectious cadavers in the environment, which

340 we symbolize as P for pathogen). Our SEIR model is modified to allow hosts to vary in
341 infection risk, an important feature of gypsy moth virus transmission (Dwyer et al. 1997; Elderd
342 et al. 2008), and to allow exposed hosts to be re-exposed, because infected gypsy moth larvae
343 continue to consume foliage until shortly before death (Eakin et al. 2014). For computational
344 convenience (Wearing et al. 2005), most SEIR models assume that the time between exposure
345 and infectiousness follows a gamma distribution (Keeling and Rohani 2008). We instead allow
346 this time to be determined by our within-host model, so that the within-host model is nested
347 inside the stochastic SEIR model. As in the within-host model, the frequency of different virus
348 strains at the population scale can drift due to chance events, such as the exposure of hosts to
349 one cadaver and not another. Our between-host model therefore adds an additional source of
350 drift to our nested models.

351 Over longer time scales, gypsy moth populations go through host-pathogen population
352 cycles, in which host outbreaks are terminated by baculovirus epizootics. This pattern
353 is typical of many forest defoliating insects (Moreau and Lucarotti 2007). The resulting
354 predator-prey-type oscillations drive gypsy moth outbreaks at intervals of 5-9 years (Dwyer
355 et al. 2004, we neglect the effects of the gypsy moth fungal pathogen *Entomophaga maimaiga*,
356 which was having only modest effects in our study areas in Michigan, USA, when we collected
357 our samples). Between insect outbreaks, virus infection rates are very low (Elder et al. 2008),
358 which may strengthen the effects of genetic drift.

359 Gypsy moths have only one generation per year, and therefore only one epizootic per year.
360 We thus nest our within-host/SEIR-type model into a model that describes host reproduction
361 and virus survival after the epizootic (fig. 1). The SEIR model determines which hosts die
362 during the epizootic and which virus strains killed those hosts. This information is used in
363 difference equations that describe the reproduction of the surviving hosts, the survival of the
364 pathogen over the winter, and the evolution of host resistance, an important factor in gypsy

365 moth outbreak cycles (Dwyer et al. 2000; Elder et al. 2008).

366 By explicitly tracking the dynamics of individual hosts and pathogens, our model inherently
367 includes the effects of genetic drift. We also tested whether a simple model of purifying
368 selection, or a model of *de novo* mutation could explain the patterns of diversity in the
369 data, without invoking drift within hosts. If these models were to fail to explain the
370 patterns of diversity seen in our data, more complex models of evolution would need to be
371 considered. In the gypsy moth baculovirus system, however, mutation rates are likely low
372 (Rohrman 2008; Sanjuán and Domingo-Calap 2016), spatial structure appears to be weak
373 (Fujita 2007, Supplemental Information A), and evidence of selection acting within hosts is
374 lacking (Supplemental Information H). Drift therefore seems likely to play a strong role in
375 shaping virus diversity.

376 To show that the different sources of drift in our model are actually necessary to explain
377 the data, we created three alternative models. All three alternative models simply the effects
378 of genetic drift, but one also allows for effects of purifying selection. For the first alternative
379 model, we simplified the effects of genetic drift by assuming that the relative frequencies of
380 different virus strains within hosts do not change during pathogen population growth within
381 hosts. To do this, we altered the model output such that the relative frequencies of virus
382 strains released from a host upon host death were equal to the relative frequencies of virus
383 strains just after the transmission bottleneck, thereby eliminating the effects of replicative drift
384 (Fig. 1). For the second alternative model, we further simplified the effects of drift by assuming
385 that the relative frequencies of virus strains at the end of an infection were the same as their
386 relative frequencies in the infectious cadaver that initiated the infection, thereby eliminating
387 both replicative drift and transmission bottlenecks (fig. 1). For the third alternative model, we
388 added purifying selection to the second alternative model, which lacked both replicative drift
389 and transmission bottlenecks. We did this by assuming that each host was susceptible to only

390 a random subset of virus strains, so that exposure would only result in death if a host was
391 susceptible to one or more virus strains in the cadaver to which it was exposed. The relative
392 frequencies of virus strains released upon death was then equal to the relative frequencies of
393 virus strains to which that host was susceptible to in the infecting cadaver.

394 **Baculovirus sequencing**

395 We collected larvae from outbreaking gypsy moth populations in Michigan between 2000 and
396 2003 (Supplemental Information A), and we reared the larvae until they pupated or died of
397 infection (Woods and Elkinton 1987). The virus population from each virus-killed larva was
398 passaged once by infecting 75 larvae with liquefied cadaver to generate enough virus for DNA
399 extraction. We then extracted DNA following a standard baculovirus DNA extraction protocol,
400 and we amplified the DNA using whole genome amplification (REPLI-g UltraFast Mini kit
401 from Qiagen).

402 We constructed sequencing libraries using the Nextera DNA Sample Prep Kit
403 (Illumina-compatible, #GA0911-96) with custom barcodes to distinguish between the virus
404 communities of different hosts. Our barcodes consisted of the first 96 indexes proposed
405 by Meyer and Kircher (2010) (Supplemental Information A). Sequencing was carried out as
406 two sets of libraries, run on individual lanes of a HiSeq2000 at the University of Illinois
407 at Urbana-Champaign, producing 100 cycle single-end reads. Samples were separated by
408 barcode using the standard Illumina pipeline, and adaptor contamination was removed using
409 ‘trim_galore’. Reads were mapped to the first sequenced gypsy moth baculovirus genome
410 (Kuzio et al. 1999) using ‘bowtie2’ (Langmead and Salzberg 2012) with parameter set
411 ‘very-fast’ (Supplemental Information A). Overall mean coverage was 886x, and varied across
412 samples from 202x to 1497x (fig. S3). Variant calling was carried out using ‘VarScan’ version
413 2.3.9 (Koboldt et al. 2012). More details can be found in Supplemental Information A.

414 **Data and code availability**

415 Sequence data generated in this study are available through the Sequence Read
416 Archive (SRA) of the National Center for Biotechnology Information (NCBI)
417 under BioProject ID PRJNA386565. Author-generated code is available at GitHub
418 repository: <https://github.com/dkenned1/KennedyDwyer>.

419 **Acknowledgements**

420 Our work was supported by NIH grant R01-GM096655 to G Dwyer, V Dukic, and B Rehill.
421 Computational support was provided by the Computing Research Institute and the Research
422 Computing Center at the University of Chicago.

423 **References**

- 424 ABEL, S., ZUR WIESCH, P. A., DAVIS, B. M., AND WALDOR, M. K. 2015. Analysis of
425 bottlenecks in experimental models of infection. *PLoS Pathog* 11:e1004823.
- 426 ALIZON, S., LUCIANI, F., AND REGOES, R. R. 2011. Epidemiological and clinical
427 consequences of within-host evolution. *Trends Microbiol* 19:24–32.
- 428 ALIZON, S. AND VAN BAALEN, M. 2008. Acute or chronic? Within-host models with immune
429 dynamics, infection outcome and parasite evolution. *Am Nat* 172:E244–E256.
- 430 ASHIDA AND BREY, P. T. 1998. Molecular Mechanisms of Immune Responses in Insects.
431 Chapman & Hall, London.
- 432 AZARIAN, T., PRESTI, A. L., GIOVANETTI, M., CELLA, E., RIFE, B., LAI, A., ZEHENDER,
433 G., CICCOCCHI, M., AND SALEMI, M. 2015. Impact of spatial dispersion, evolution, and
434 selection on Ebola Zaire Virus epidemic waves. *Sci Rep* 5.
- 435 CHATEIGNER, A., BÉZIER, A., LABROUSSE, C., JOLLE, D., BARBE, V., AND HERNIOU,
436 E. A. 2015. Ultra deep sequencing of a baculovirus population reveals widespread genomic
437 variations. *Viruses* 7:3625–3646.
- 438 DIDELOT, X., GARDY, J., AND COLIJN, C. 2014. Bayesian inference of infectious disease
439 transmission from whole-genome sequence data. *Mol Biol Evol* 31:1869–1879.

- 440 DWYER, G., DUSHOFF, J., ELKINTON, J. S., AND LEVIN, S. A. 2000. Pathogen-driven
441 outbreaks in forest defoliators revisited: Building models from experimental data. *Am Nat*
442 156:105–120.
- 443 DWYER, G., DUSHOFF, J., AND YEE, S. H. 2004. The combined effects of pathogens and
444 predators on insect outbreaks. *Nature* 430:341–345.
- 445 DWYER, G., ELKINTON, J. S., AND BUONACCORSI, J. P. 1997. Host heterogeneity in
446 susceptibility and disease dynamics: Tests of a mathematical model. *Am Nat* 150:685–707.
- 447 EAKIN, L., WANG, M., AND DWYER, G. 2014. The effects of the avoidance of infectious
448 hosts on infection risk in an insect-pathogen interaction. *Am Nat* 185:100–112.
- 449 ELDERD, B. D. 2013. Developing models of disease transmission: insights from ecological
450 studies of insects and their baculoviruses. *PLoS Pathog* 9:e1003372.
- 451 ELDERD, B. D., DUSHOFF, J., AND DWYER, G. 2008. Host-pathogen interactions, insect
452 outbreaks, and natural selection for disease resistance. *Am Nat* 172:829–842.
- 453 ELDERD, B. D., REHILL, B. J., HAYNES, K. J., AND DWYER, G. 2013. Induced plant
454 defenses, host–pathogen interactions, and forest insect outbreaks. *P Natl Acad Sci USA*
455 110:14978–14983.
- 456 ELKINTON, J. S. AND LIEBHOLD, A. M. 1990. Population dynamics of gypsy moth in North
457 America. *Annu Rev Entomol* 35:571–596.
- 458 FLEMING-DAVIES, A. E. AND DWYER, G. 2015. Phenotypic variation in overwinter
459 environmental transmission of a baculovirus and the cost of virulence. *Am Nat* 186:797–806.
- 460 FROST, S. D., PYBUS, O. G., GOG, J. R., VIBOUD, C., BONHOEFFER, S., AND BEDFORD,
461 T. 2015. Eight challenges in phylodynamic inference. *Epidemics* 10:88–92.
- 462 FUJITA, P. A. 2007. Combining models with empirical data to examine dispersal mechanisms
463 in the gypsy moth nucleopolyhedrosis host-pathogen system. Ph.D. dissertation, University
464 of Chicago.
- 465 FULLER, E., ELDERD, B. D., AND DWYER, G. 2012. Pathogen persistence in the environment
466 and insect-baculovirus interactions: disease-density thresholds, epidemic burnout and insect
467 outbreaks. *Am Nat* 179.
- 468 GOG, J. R., PELLIS, L., WOOD, J. L., MCLEAN, A. R., ARINAMINPATHY, N., AND
469 LLOYD-SMITH, J. O. 2015. Seven challenges in modeling pathogen dynamics within-host
470 and across scales. *Epidemics* 10:45–48.

- 471 GRENFELL, B. T., PYBUS, O. G., GOG, J. R., WOOD, J. L. N., DALY, J. M., MUMFORD,
472 J. A., AND HOLMES, E. C. 2004. Unifying the epidemiological and evolutionary dynamics
473 of pathogens. *Science* 303:327–332.
- 474 GUTIÉRREZ, S., MICHALAKIS, Y., AND BLANC, S. 2012. Virus population bottlenecks
475 during within-host progression and host-to-host transmission. *Curr Opin Virol* 2:546–555.
- 476 HATHERELL, H.-A., COLIJN, C., STAGG, H. R., JACKSON, C., WINTER, J. R., AND
477 ABUBAKAR, I. 2016. Interpreting whole genome sequencing for investigating tuberculosis
478 transmission: a systematic review. *BMC Med* 14:1.
- 479 HODGSON, D. J., VANBERGEN, A. J., WATT, A. D., HAILS, R. S., AND CORY, J. S. 2001.
480 Phenotypic variation between naturally co-existing genotypes of a Lepidopteran baculovirus.
481 *Evol Ecol Res* 3:687–701.
- 482 HUDSON, A. I., FLEMING-DAVIES, A. E., PÁEZ, D. J., AND DWYER, G. 2016.
483 Genotype-by-genotype interactions between an insect and its pathogen. *J Evolution Biol*
484 29:2480–2490.
- 485 KEELING, M. J. AND ROHANI, P. 2008. Modeling Infectious Diseases. Princeton University
486 Press, New Jersey.
- 487 KENNEDY, D. A., DUKIC, V., AND DWYER, G. 2014. Pathogen growth in insect hosts:
488 inferring the importance of different mechanisms using stochastic models and response-time
489 data. *Am Nat* 184:407–423.
- 490 KENNEDY, D. A., DUKIC, V., AND DWYER, G. 2015. Combining principal component
491 analysis with parameter line-searches to improve the efficacy of Metropolis–Hastings
492 MCMC. *Environ Ecol Stat* 22:247–274.
- 493 KLINKENBERG, D., BACKER, J. A., DIDELOT, X., COLIJN, C., AND WALLINGA, J.
494 2017. Simultaneous inference of phylogenetic and transmission trees in infectious disease
495 outbreaks. *PLoS Comput Biol* 13:e1005495.
- 496 KOBOLDT, D. C., ZHANG, Q., LARSON, D. E., SHEN, D., MCLELLAN, M. D., LIN, L.,
497 MILLER, C. A., MARDIS, E. R., DING, L., AND WILSON, R. K. 2012. VarScan 2: somatic
498 mutation and copy number alteration discovery in cancer by exome sequencing. *Genome Res*
499 22:568–576.
- 500 KOELLE, K., COBEY, S., GRENFELL, B., AND PASCUAL, M. 2006. Epochal evolution shapes
501 the phylodynamics of inter-pandemic influenza a (H3N2) in humans. *Science* 314:1898–1903.
- 502 KOT, M. 2001. Elements of Mathematical Ecology. Cambridge University Press, Cambridge.

- 503 KOUYOS, R. D., ALTHAUS, C. L., AND BONHOEFFER, S. 2006. Stochastic or deterministic:
504 what is the effective population size of HIV-1? *Trends Microbiol* 14:507–511.
- 505 KUZIO, J., PEARSON, M. N., HARWOOD, S. H., FUNK, C. J., EVANS, J. T., SLAVICEK,
506 J. M., AND ROHRMANN, G. F. 1999. Sequence and analysis of the genome of a baculovirus
507 pathogenic for *Lymantria dispar*. *Virology* 253:17–34.
- 508 LANGMEAD, B. AND SALZBERG, S. L. 2012. Fast gapped-read alignment with bowtie 2. *Nat*
509 *Methods* 9:357–359.
- 510 LEE, R. S., RADOMSKI, N., PROULX, J.-F., LEVADE, I., SHAPIRO, B. J., MCINTOSH,
511 F., SOUALHINE, H., MENZIES, D., AND BEHR, M. A. 2015. Population genomics of
512 mycobacterium tuberculosis in the inuit. *Proc Natl Acad Sci USA* 112:13609–13614.
- 513 LIPKIN, W. I. AND ANTHONY, S. J. 2015. Virus hunting. *Virology* 479:194–199.
- 514 LORENZO-REDONDO, R., FRYER, H. R., BEDFORD, T., KIM, E.-Y., ARCHER, J., POND, S.
515 L. K., CHUNG, Y.-S., PENUGONDA, S., CHIPMAN, J. G., FLETCHER, C. V., SCHACKER,
516 T. W., MALIM, M. H., RAMBAUT, A., HAASE, A. T., MCLEAN, A. R. ., AND WOLINSKY,
517 S. M. 2016. Persistent HIV-1 replication maintains the tissue reservoir during therapy. *Nature*
518 530:51+.
- 519 MALDARELLI, F., KEARNEY, M., PALMER, S., STEPHENS, R., MICAN, J., POLIS,
520 M. A., DAVEY, R. T., KOVACS, J., SHAO, W., ROCK-KRESS, D., ET AL. 2013. HIV
521 populations are large and accumulate high genetic diversity in a nonlinear fashion. *J Virol*
522 87:10313–10323.
- 523 MEYER, M. AND KIRCHER, M. 2010. Illumina sequencing library preparation for highly
524 multiplexed target capture and sequencing. *Cold Spring Harb Protoc* 2010:1–10.
- 525 MIDEO, N., ALIZON, S., AND DAY, T. 2008. Linking within-and between-host dynamics in
526 the evolutionary epidemiology of infectious diseases. *Trends Ecol Evol* 23:511–517.
- 527 MIDEO, N., BAILEY, J. A., HATHAWAY, N. J., NGASALA, B., SAUNDERS, D. L., LON, C.,
528 KHARABORA, O., JAMNIK, A., BALASUBRAMANIAN, S., BJÖRKMAN, A., ET AL. 2016.
529 A deep sequencing tool for partitioning clearance rates following antimalarial treatment in
530 polyclonal infections. *Evol Med Public Health* 2016:21–36.
- 531 MOREAU, G. AND LUCAROTTI, C. J. 2007. A brief review of the past use of baculoviruses
532 for the management of eruptive forest defoliators and recent developments on a sawfly virus
533 in canada. *Forest Chron* 83:105–112.
- 534 MURRAY, K. D. AND ELKINTON, J. S. 1989. Environmental contamination of egg
535 masses as a major component of transgenerational transmission of gypsy-moth nuclear
536 polyhedrosis-virus (LdMNPV). *J Invertebr Pathol* 53:324–334.

- 537 NAGYLAKI, T. 1992. Introduction to Theoretical Population Genetics. Springer-Verlag, Berlin
538 Heidelberg.
- 539 NEI, M. AND LI, W. H. 1979. Mathematical model for studying genetic variation in terms of
540 restriction endonucleases. *Proc Natl Acad Sci USA* 76:5269–5273.
- 541 ORR, H. A. 1998. Testing natural selection vs. genetic drift in phenotypic evolution using
542 quantitative trait locus data. *Genetics* 149:2099–2104.
- 543 PENNINGS, P. S., KRYAZHIMSKIY, S., AND WAKELEY, J. 2014. Loss and recovery of genetic
544 diversity in adapting populations of HIV. *PLoS Genet* 10:e1004000.
- 545 READ, A. F. AND TAYLOR, L. H. 2001. The ecology of genetically diverse infections. *Science*
546 292:1099–1102.
- 547 RENSHAW, E. 1991. Modeling Biological Populations in Space and Time. Cambridge
548 University Press, Cambridge.
- 549 ROHRMANN, G. F. 2008. Baculovirus Molecular Biology. National Library of Medicine (US),
550 Bethesda.
- 551 SAATY, T. L. 1961. Some stochastic-processes with absorbing barriers. *J R Stat Soc Series B*
552 *Stat Methodol* 23:319–334.
- 553 SANJUÁN, R. AND DOMINGO-CALAP, P. 2016. Mechanisms of viral mutation. *Cell Mol Life*
554 *Sci* 73:4433–4448.
- 555 SOBEL LEONARD, A., WEISSMAN, D., GREENBAUM, B., GHEDIN, E., AND KOELLE, K.
556 2017. Transmission bottleneck size estimation from pathogen deep-sequencing data, with an
557 application to human influenza A virus. *J Virol* pp. JVI–00171.
- 558 TRUDEAU, D., WASHBURN, J. O., AND VOLKMAN, L. E. 2001. Central role of hemocytes
559 in *Autographa californica* M nucleopolyhedrovirus pathogenesis in *Heliothis virescens* and
560 *Helicoverpa zea*. *J Virol* 75:996–1003.
- 561 VIGNUZZI, M., STONE, J. K., ARNOLD, J. J., CAMERON, C. E., AND ANDINO, R. 2006.
562 Quasispecies diversity determines pathogenesis through cooperative interactions in a viral
563 population. *Nature* 439:344–348.
- 564 VILMOS, P. AND KURUCZ, E. 1998. Insect immunity: Evolutionary roots of the mammalian
565 innate immune system. *Immunol Lett* 62:59–66.
- 566 VOLZ, E. M., ROMERO-SEVERSON, E., AND LEITNER, T. 2017. Phylodynamic inference
567 across epidemic scales. *Mol Biol Evol* 34:1276–1288.

- 568 WEARING, H. J., ROHANI, P., AND KEELING, M. J. 2005. Appropriate models for the
569 management of infectious diseases. *PLoS Med* 2:e174.
- 570 WILSON, M. R., NACCACHE, S. N., SAMAYOA, E., BIAGTAN, M., BASHIR, H., YU,
571 G., SALAMAT, S. M., SOMASEKAR, S., FEDERMAN, S., MILLER, S., ET AL. 2014.
572 Actionable diagnosis of neuroleptospirosis by next-generation sequencing. *New Engl J Med*
573 370:2408–2417.
- 574 WOODS, S. A. AND ELKINTON, J. S. 1987. Bimodal patterns of mortality from nuclear
575 polyhedrosis-virus in gypsy-moth (*Lymantria-dispar*) populations. *J Invertebr Pathol*
576 50:151–157.
- 577 YPMA, R. J., VAN BALLEGOIJEN, W. M., AND WALLINGA, J. 2013. Relating phylogenetic
578 trees to transmission trees of infectious disease outbreaks. *Genetics* 195:1055–1062.
- 579 ZWART, M. P., HEMERIK, L., CORY, J. S., DE VISSER, J. A. G. M., BIANCHI, F. J. J. A.,
580 VAN OERS, M. M., VLAK, J. M., HOEKSTRA, R. F., AND VAN DER WERF, W. 2009. An
581 experimental test of the independent action hypothesis in virus-insect pathosystems. *Proc R*
582 *Soc Lond B* 276:2233–2242.

583 **Figure 1:** Schematic of the nested model. Bottom, the host population size N_g and the
584 infectious cadaver population size Z_g in generation g depend on host and pathogen population
585 sizes in generation $g - 1$ and the disease dynamics in that generation. Following the epizootic,
586 surviving hosts reproduce and virus-killed cadavers overwinter at rate ϕ to start the epizootic
587 in the following year. Middle, the disease dynamics in generation $g - 1$ follow a stochastic
588 SEIR model (Keeling and Rohani 2008), such that a susceptible host S_i becomes exposed E_j
589 to infectious cadaver P_k at rate $\nu_i q$, where ν_i is the risk of exposure for host i and q is the
590 probability of death given exposure, which arises from the within host virus dynamics. Note
591 that the “Removed” class R , corresponding to inactivated cadavers, is not explicitly shown.
592 The probability of a host dying from virus infection at time τ post exposure $p(\tau)$, is determined
593 by the dynamics of the pathogen within a host. q is related to $p(\tau)$ in that $q = \int_0^\infty p(\tau) d\tau$. Top,
594 within a host, virus particles x can reproduce or interact with immune cells y , resulting in the
595 removal of both the virus particle and the immune cell. An infection fails to kill the host if all
596 virus particles are cleared so that $x = 0$, but the host dies if the total number of virus particles
597 reaches an upper threshold C . Further details are in Supplemental Information C. To produce
598 a model that lacks replicative drift, we assume that the frequency of a virus strain l at time of
599 death τ , $f_l(\tau)$, is equal to the frequency of that strain immediately after the time of exposure
600 $f_l(0)$. To produce a model that lacks transmission bottlenecks, we assume that the number of
601 copies of a virus strain l at the beginning of an infection $x_l(0)$ is equal to the total number of
602 virus particles that invade the host $\sum_l x_l(0)$, times the relative frequency of that virus strain in
603 the cadaver that caused exposure $P_l / (\sum_p P_p)$. In the model that lacks transmission bottlenecks
604 and replicative drift, host death occurs only if a larva was susceptible to one or more of the
605 virus strains in the cadaver to which it was exposed. If so, the virus strains that the host was
606 susceptible to are released upon host death at frequencies equal to those in the infecting cadaver.

607

608 **Figure 2:** Simulations of the nested model. In all panels (A)-(F), colored curves represent
609 the pathogen population sizes of different virus strains, and the black curve shows the
610 total pathogen population size. The colored bar at the top of each panel shows the relative
611 frequencies of virus strains over time. Panels (A)-(C) show three realizations of the within-host
612 virus growth model. A re-exposure event, marked by a dashed, vertical red line, is also shown
613 in panel (C). The top colored panel left of time 0 shows the frequency of virus strains in a
614 cadaver that a host was exposed to at time 0 (and re-exposed to at time 50 in panel (C)). Death
615 occurs when the total number of virus particles within a host hits an upper threshold. To aid
616 visualization, here we set the pathogen population size at host death to be 10^4 , as opposed
617 to the more realistic value of 10^9 that we use when comparing our models to data. The time
618 of death differs between simulations due to demographic stochasticity in virus growth, and
619 in each simulation it is marked by a dashed, vertical black line. Panels (D) and (E) show
620 two realizations of our stochastic SEIR-type epizootic model starting from identical initial
621 conditions. Note that the curves here show cadaver quantities, rather than virus particles
622 as in panels (A)-(C). Epizootics are initiated by overwintered cadavers that infect emerging
623 larvae. As these cadavers decay, total cadaver quantity drops to low levels, such that the
624 pathogen population is almost entirely composed of virus particles inside living hosts. These
625 hosts then die initiating future rounds of infections. Panel (F) shows a realization of our
626 between-generation pathogen model, with trajectories showing the total number of virus-killed
627 hosts in each generation. The frequency of pathogen strains can drift over time, an effect that is
628 particularly noticeable during troughs of infection.

629

630 **Figure 3:** Comparison of the predictions of our models (gray-shaded areas, showing 95
631 percent confidence intervals of model realizations) to the distribution of nucleotide diversity
632 within 143 individual infected hosts calculated from our sequence data (black dots show

633 data on nucleotide diversity within hosts). (A) shows the predictions of a model that lacks
634 both transmission bottlenecks and replicative drift, (B) shows the predictions of a model that
635 includes transmission bottlenecks but not replicative drift, (C) shows the predictions of a model
636 that includes both transmission bottlenecks and replicative drift, and (D) shows the predictions
637 of a model that includes purifying selection within hosts but not transmission bottlenecks or
638 replicative drift.

639

640 **Figure 4:** Representative distributions of allele frequencies from individual hosts in our best
641 model (A-E) and in our data (F-J). Each plot shows the distribution of allele frequencies within
642 a single individual at 712 segregating sites, showing only the frequency of the most common
643 allelic variant at each locus within that host. The number on each plot is the mean nucleotide
644 diversity within that particular host. Model plots are aligned with similar data plots. The lack
645 of diversity in panels A and F suggests that the virus population within these hosts consist of
646 only a single virus strain. The bimodal distributions in panels B, C and G suggest that these
647 virus populations contain exactly two virus strains. The high diversity but lack of bimodality
648 in panels D, E, H, I, and J suggests that these virus populations consist of more than two virus
649 strains.

650

651 **Figure 5:** Model predictions of the effects of changes in the populations of susceptible and
652 infected hosts on within-host pathogen diversity, over the host-pathogen population cycle. (A)
653 The population size of uninfected hosts. (B) The population size of infectious cadavers (blue)
654 and the mean nucleotide diversity (red).

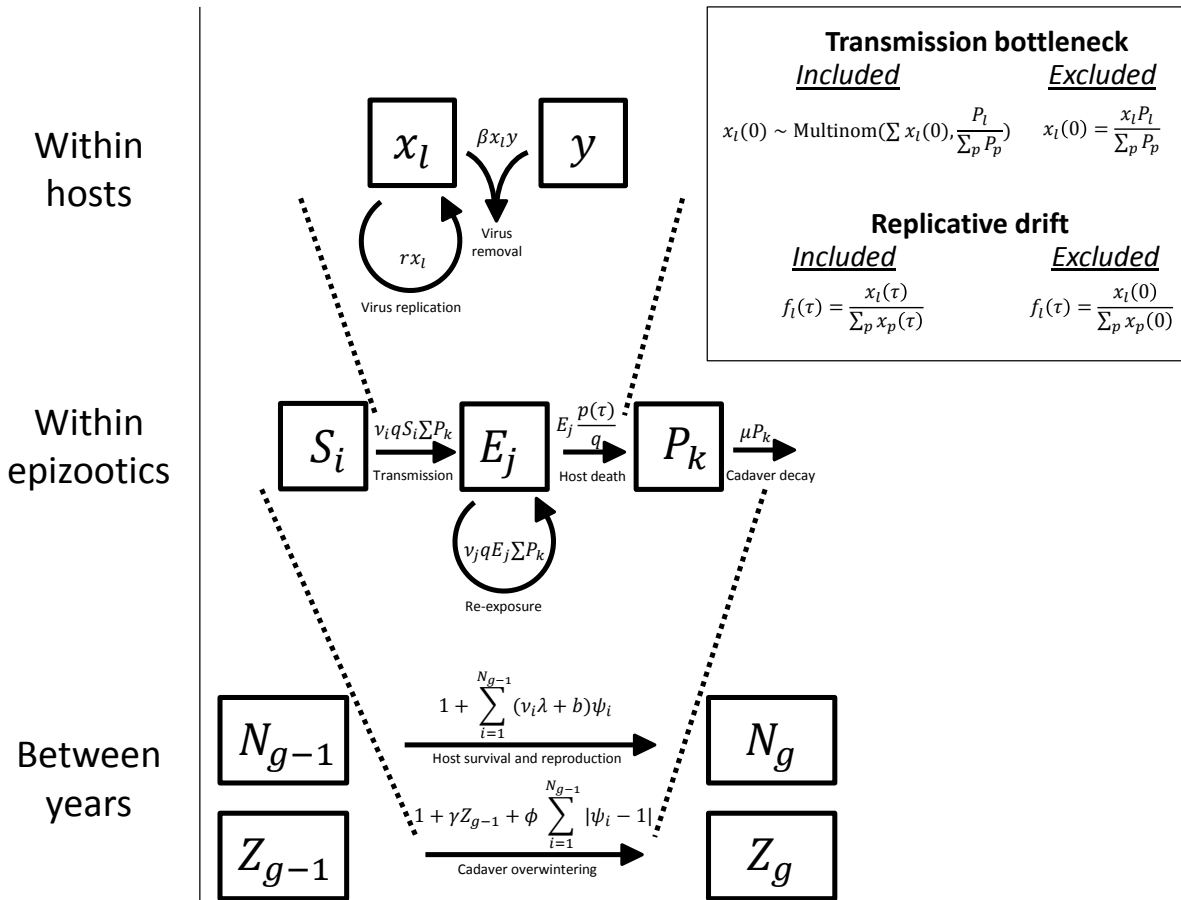


Figure 1

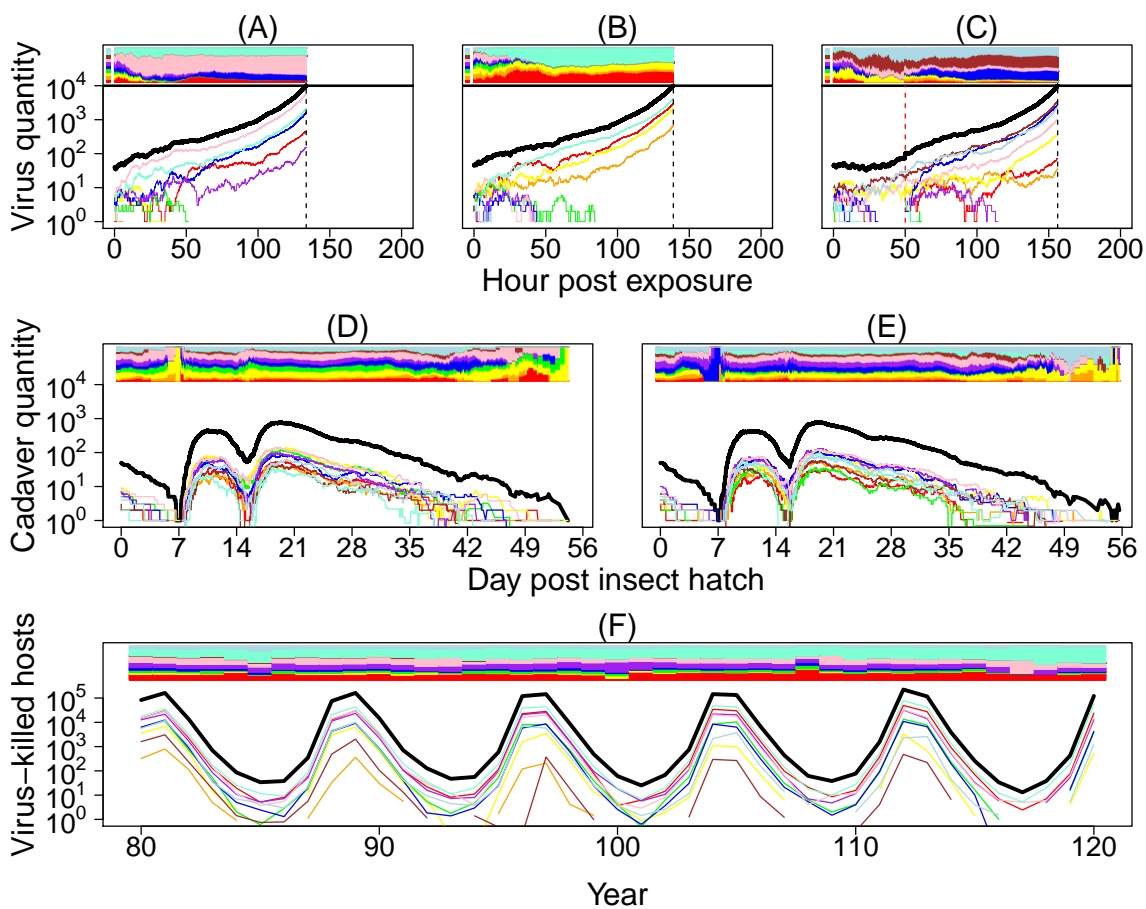


Figure 2

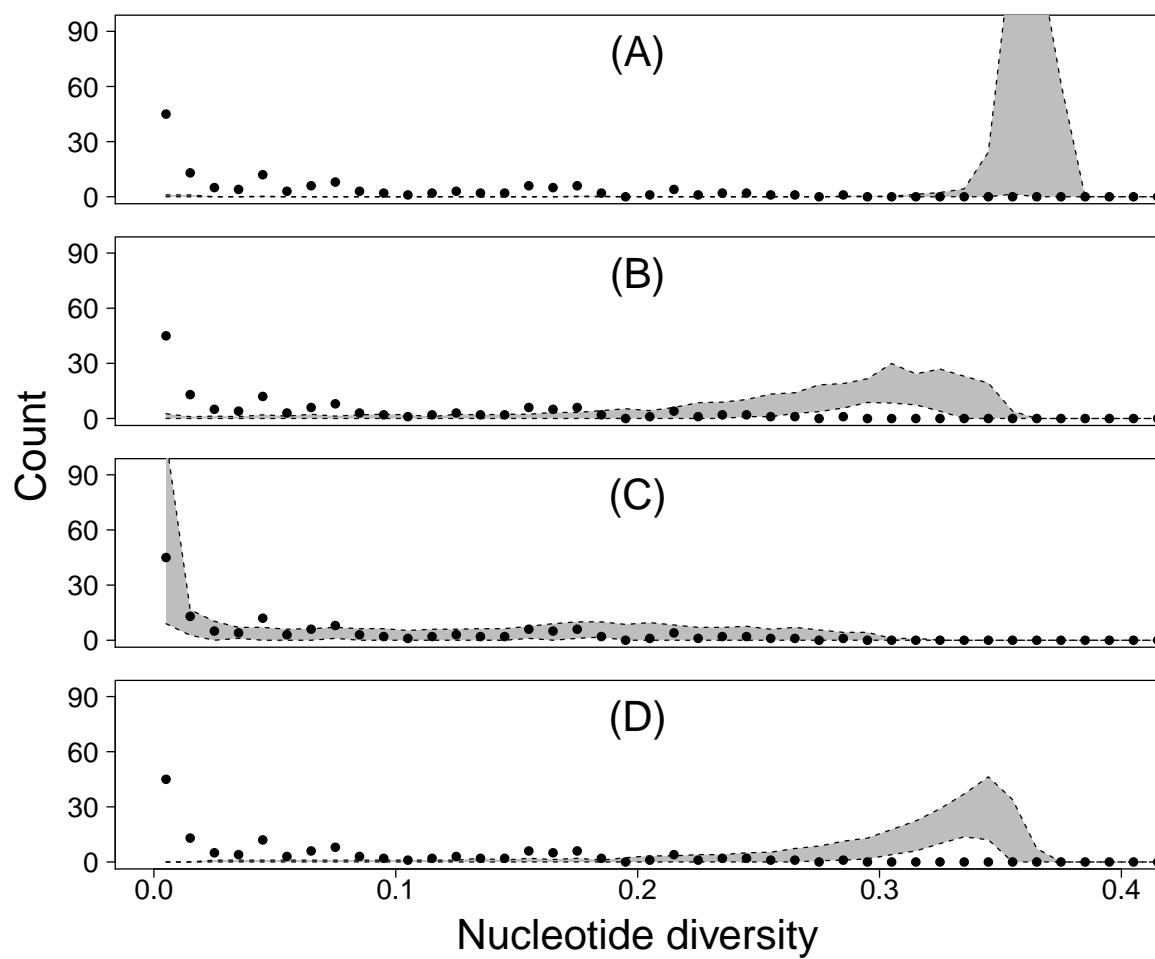


Figure 3

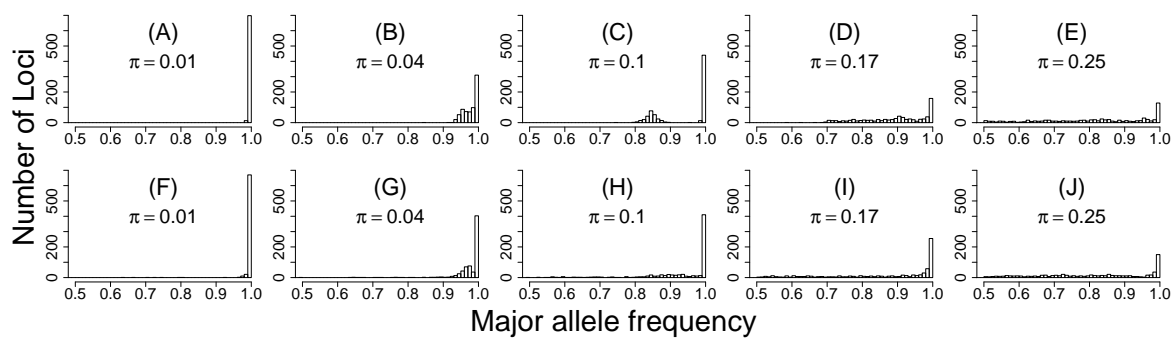


Figure 4

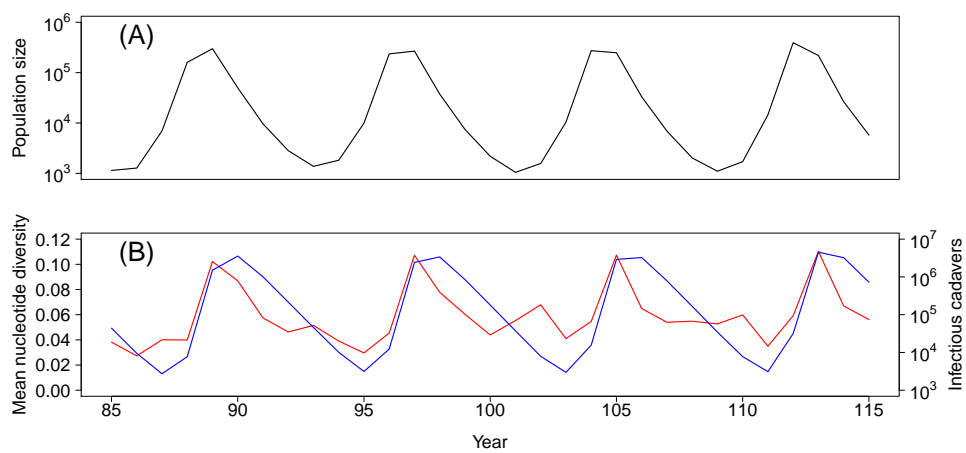


Figure 5